

the bands at 292/302 (aza nitrogens<sup>22</sup>) 228/257-241, and 126/98-115  $\text{cm}^{-1}$  (Zn-N(macrocycle)), the  $\alpha$  and  $\beta$  modifications frequencies being respectively before and behind the slash. As these two forms differ only by the relative position of Pc planes, vibrations in  $\beta$ -ZnPc could be given as more sensitive to axial N(aza)-Zn interactions between adjacent molecules in the herringbone stacking. The same group of bands is much more altered in ZnPcCl. Considerable broadening or loss of intensity as well as frequency shifts is evident at 421, 341, 126, and 88  $\text{cm}^{-1}$ . Three bands at 302, 261, and 246  $\text{cm}^{-1}$  nearly vanish. Two rather important and well-defined bands at 277 and 213  $\text{cm}^{-1}$  are good candidates for Zn-Cl stretching modes.<sup>20</sup> This would be consistent with the weak axial bond on Zn, characterized in the lattice cell. Spectra of the similar compounds ZnPcX (X  $\neq$  Cl) are currently being studied in our group and will help assign the absorptions in the low-frequency region for the stacked compounds of this series.

### Conclusion

Our investigation answers diverse proposals on the structure of ZnPcCl.<sup>20</sup> We have prepared this compound by an original procedure, rarely applied to this class of molecules, for which partial oxidation through iodine insertion looks to be the general

way of access to semiconductive or metallic molecular material. FT-IR results are consistent with X-ray analysis data.

ZnPcCl owes its electrical properties (i) to the integral oxidation number of the bimolecular entity (ZnPc)<sub>2</sub>, (ii) to the very close association and favorable staggering angle of Pc rings, (iii) to the limited but effective interaction between the aromatic rings of the (ZnPc)<sub>2</sub> blocks in the helical stacking, and (iv) to the limited mobility of the counteranions. This first example of undoped Pc semiconductors displays a distinct structural feature: the metal atom lies at a distance of 0.59 Å from the ring center. For similar complexes, the metal atom displacement from the ring center is always much smaller.

The main character of higher conductivity and lower activation energy is being investigated on the same type of ZnPcX crystals, electrodeposited in the presence of NR<sub>4</sub><sup>+</sup>X<sup>-</sup> electrolytes. Improvements of preparative conditions are expected to yield large enough single crystals to perform a full study of the anisotropy.

Registry No. ZnPcCl, 53466-59-4.

**Supplementary Material Available:** Listings of structure factor amplitudes, root-mean-square amplitudes of thermal vibration, general temperature factor expressions (*U*'s), and torsional angles (in degrees) (7 pages). Ordering information is given on any current masthead page.

Contribution from the Department of Chemistry,  
Purdue University, West Lafayette, Indiana 47907

## Ligand Structural Influences upon Electrochemical Reactivity: Organic Substituent Effects upon (Carboxylato)pentaamminecobalt(III) Reductions at Mercury and Gold Electrodes

TOMI T.-T. LI and MICHAEL J. WEAVER\*

Received October 12, 1984

The electroreduction kinetics of 33 (carboxylato)pentaamminecobalt(III) complexes containing a variety of aliphatic, aromatic, and heterocyclic substituents have been examined at mercury- and gold-aqueous interfaces and compared with the corresponding homogeneous reduction rates with Ru(NH<sub>3</sub>)<sub>6</sub><sup>2+</sup> in order to examine the relationships between the substituent structure and electrochemical reactivity. Complexes having acyclic aliphatic groups yielded "normal" outer-sphere reactivities on the basis of their similar relative rate constants at a given electrode potential in comparison with the corresponding homogeneous rate ratios. However, electrochemical reactivities that are enhanced by ca. 10-10<sup>4</sup>-fold on this basis were observed for complexes with ring-containing substituents. The extent of these rate enhancements depended on the ring structure, the smallest (ca. 10-30-fold) being seen with aliphatic ring substituents and the largest (200-10<sup>3</sup>-fold) for thiophenes, with intermediate values for reactants having furan, pyridine, and benzene groups. Similar unimolecular rate constants were nonetheless observed for the electroreduction of several of these complexes when electrostatically adsorbed at chloride-coated silver. This indicates that the observed catalysis at mercury and gold surfaces arises from reactant adsorption, i.e., from increased precursor stability, presumably associated with "hydrophobic" or van der Waals ligand-surface interactions. "Normal" outer-sphere electroreduction pathways were observed, however, at mercury electrodes in several aprotic solvents, as deduced from the common correlation between the electrochemical reactivities and the inductive substituent parameter. A similar correlation is seen for the Ru(NH<sub>3</sub>)<sub>6</sub><sup>2+</sup> reduction kinetics in aqueous solution.

### Introduction

We have recently been examining the kinetics of simple electrochemical reactions involving transition-metal systems, primarily Co(III)/Co(II), Cr(III)/Cr(II), and Ru(III)/Ru(II) couples at a variety of metal-solution interfaces.<sup>1</sup> One objective is to evaluate how the rates and mechanisms of heterogeneous electron-transfer reactions are influenced by the coordinated ligand structure, especially in relation to the detailed picture of reactant structural effects that has emerged for reactions between metal complexes in homogeneous solution.<sup>2</sup> Similarly to homogeneous processes,

such electrochemical reactions commonly occur via inner-sphere mechanisms where a coordinated ligand is bound directly in the transition state for electron transfer.<sup>2a</sup> Not surprisingly, the kinetics of such inner-sphere reactions are often extremely sensitive to both the nature of the metal surface and to the bridging ligand.<sup>1f-h,2c</sup>

By analogy with homogeneous processes, outer-sphere electrochemical mechanisms are anticipated for reactants that lack a functional group capable of binding to the metal surface. Thus, electron transfer involving such species is expected to occur without the coordinated ligands penetrating the inner layer of solvent molecules adjacent to the electrode surface (the electrode's "coordination layer").<sup>2a</sup> One therefore might expect that the

(1) For example, see the following and references cited therein: (a) Barr, S. W.; Guyer, K. L.; Weaver, M. J. *J. Electroanal. Chem. Interfacial Electrochem.* **1980**, *111*, 41. (b) Weaver, M. J. *J. Phys. Chem.* **1980**, *84*, 568. (c) Weaver, M. J.; Tyma, P. D.; Nettles, S. M. *J. Electroanal. Chem. Interfacial Electrochem.* **1980**, *114*, 53. (d) Srinivasan, V.; Barr, S. W.; Weaver, M. J. *Inorg. Chem.* **1982**, *21*, 3154. (e) Hupp, J. T.; Weaver, M. J. *Inorg. Chem.* **1983**, *22*, 2557. (f) Barr, S. W.; Weaver, M. J. *Inorg. Chem.* **1984**, *23*, 1657. (g) Guyer, K. L.; Weaver, M. J. *Inorg. Chem.* **1984**, *23*, 1657. (h) Li, T. T.-T.; Liu, H. Y.; Weaver, M. J. *J. Am. Chem. Soc.* **1984**, *106*, 1233.

(2) (a) Weaver, M. J. *Isr. J. Chem.* **1979**, *18*, 35. (b) Weaver, M. J.; Hupp, J. T. *ACS Symp. Ser.* **1982**, *No. 198*, 181. (c) Barr, S. W.; Guyer, K. L.; Li, T. T.-T.; Liu, H. Y.; Weaver, M. J. *J. Electrochem. Soc.* **1984**, *131*, 1626. (d) Hupp, J. T.; Liu, H. Y.; Farmer, J. K.; Gennett, T.; Weaver, M. J. *J. Electroanal. Chem. Interfacial Electrochem.* **1984**, *168*, 313. (e) Hupp, J. T.; Weaver, M. J. *J. Phys. Chem.*, in press.

reactant-electrode interactions for such pathways would be weak and nonspecific, such that the reaction energetics would be essentially unaffected by the interfacial environment.

A useful way of testing this notion is to examine the sensitivity of the electrochemical reactivities to variations in the ligand structure at a given electrode potential,  $E$ , in comparison with the corresponding relative homogeneous reactivities obtained using a fixed outer-sphere reducing (or oxidizing) agent,  $X$ .<sup>1b-d,f,h,2b,c,3</sup> Providing outer-sphere pathways are uniformly followed, we expect that<sup>4</sup>

$$(\Delta \log k_{\text{cor}}^e)_E = (\Delta \log k_{\text{cor}}^h)_X \quad (1)$$

where  $\Delta \log k_{\text{cor}}^e$  and  $\Delta \log k_{\text{cor}}^h$  are the corresponding variations in the work-corrected electrochemical and homogeneous rate constants, respectively. Although reasonable accordance with eq 1 has been found for a number of systems, substantial deviations have also been observed.<sup>1b-d,2b</sup>

Of particular interest are the rate variations induced by the presence of organic substituents. We have found that the substitution of the aquo ligand in  $\text{Co}(\text{NH}_3)_5\text{OH}_2^{3+}$  by 4,4'-bipyridine and related nitrogen heterocyclic ligands yields substantial (up to  $10^4$ -fold) enhancements of the Co(III) reduction rates at mercury-, platinum-, and gold-aqueous interfaces in comparison to their relative homogeneous outer-sphere reactivities, even though several of these ligands lack an effective surface-binding group.<sup>1d</sup> This behavior appears to be due to reactant adsorption induced by the relatively "hydrophobic" organic ligands.<sup>1d</sup>

We have recently employed a variety of aromatic and aliphatic carboxylate ligands bound to pentaamminecobalt(III) and containing a sulfur surface-binding group in order to examine the dependence of the unimolecular rate parameters for reduction of surface-attached Co(III) upon the structure of the extended organic bridging group.<sup>1h,2c,5</sup> A valuable feature of such  $\text{Co}(\text{NH}_3)_5\text{L}^{2+}$  reduction reactions is that wide variations in the extent of reactant-surface interactions can be achieved by altering remote substituents in the carboxylate ligand L, thereby maintaining the cobalt redox environment roughly constant. Such systems have received detailed attention in homogeneous solution.<sup>5</sup> Not surprisingly,  $\text{Co}^{III}(\text{NH}_3)_5\text{L}$  complexes containing ligands suitable for surface attachment such as thiophenecarboxylates<sup>1h</sup> yield observed electrochemical rate constants,  $k_{\text{ob}}$  ( $\text{cm s}^{-1}$ ), that are typically ca.  $10^3$ - $10^4$ -fold larger than for related reactants such as  $\text{Co}(\text{NH}_3)_5\text{OAc}^{2+}$  (OAc = acetate) that lack such binding groups.<sup>1h</sup> However, we have also observed large values of  $k_{\text{ob}}$  for other  $\text{Co}^{III}(\text{NH}_3)_5\text{L}$  complexes at mercury and gold electrodes, where L contains an extended organic functional group such as furans<sup>1h</sup> that are not expected to bind strongly to these surfaces.

We describe here a systematic examination of the electroreduction kinetics of 33  $\text{Co}(\text{NH}_3)_5\text{L}^{2+}$  complexes containing a variety of organic-substituted carboxylates, L, at mercury and gold electrodes. The aim is to ascertain broad relationships between the electrocatalytic properties (i.e.,  $k_{\text{ob}}$  enhancements) and the structural features of L. Comparisons are presented between the electrochemical reactivities at mercury and gold electrodes and rate constants for the corresponding homogeneous reactions in aqueous solution with the outer-sphere reductant  $\text{Ru}(\text{NH}_3)_6^{2+}$ . Electrochemical rate data are also presented in dimethyl sulfoxide ( $\text{Me}_2\text{SO}$ ), *N,N*-dimethylformamide (DMF), formamide, and propylene carbonate in order to examine further the influence of reactant-solvent interactions upon the reactivity patterns.

### Experimental Section

(Carboxylato)pentaamminecobalt(III) perchlorates not available from previous studies<sup>1h,5</sup> were prepared either from aquopentaamminecobalt-

(III) perchlorate in aqueous solution or from (carbonato)pentaamminecobalt(III) nitrate in diethylene glycol by utilizing the procedures outlined in ref 1h and 7, respectively. The carboxylate ligands were all obtained from Aldrich Chemical Co. Where necessary, the compounds were purified by chromatographic separation using Biogel P-2 anion resin to remove unreacted ligand, eluted with water, and recrystallized from water. The purity was confirmed by elemental analysis and infrared and UV-visible spectra. Water was purified by using a Milli Q system (Millipore, Inc.). Sodium perchlorate supporting electrolyte (G. F. Smith) was twice recrystallized from water.

Most nonaqueous solvents (Burdick and Jackson, UV grade) were degassed and stored over molecular sieves before use. Tetraethylammonium perchlorate (G. F. Smith, Co.), used as the supporting electrolyte in nonaqueous media, was recrystallized twice from water and dried in a vacuum oven.

Most observed rate constants,  $k_{\text{ob}}$  ( $\text{cm s}^{-1}$ ), were determined as a function of electrode potential,  $E$ , at both dropping-mercury and gold electrodes for ca. 1 mM reactant concentrations by means of normal-pulse polarography using a PAR 174A polarographic analyzer as outlined in ref 1a, g, and h. The gold electrode measurements utilized a rotating-disk arrangement spun at 250-500 rpm to eliminate the effect of reactant depletion from the preceding pulse.<sup>1g</sup> Some rate constants were determined additionally by using either dc polarography or rotating-disk voltammetry, the latter with rotation speeds between 100 and 2000 rpm. The gold surfaces were pretreated as in ref 1a. The resulting values of  $k_{\text{ob}}$  at gold were typically reproducible to  $\pm 50\%$ , whereas those at mercury could be reproduced to at least  $\pm 20\%$ .

Unimolecular rate constants,  $k_{\text{et}}$  ( $\text{s}^{-1}$ ), were obtained for some outer-sphere reactants by means of rapid linear sweep voltammetry, the complexes being adsorbed electrostatically at halide-coated silver surfaces, as detailed in ref 8 (see Results and Discussion). Second-order rate constants,  $k_{\text{Ru}}$  ( $\text{M}^{-1} \text{s}^{-1}$ ), for the outer-sphere reduction of the Co(III) complexes by  $\text{Ru}(\text{NH}_3)_6^{2+}$  in homogeneous solution were determined by using a polarographic method in 0.05 M sodium trifluoroacetate containing 5-20 mM trifluoroacetic acid as outlined in ref 1h.

All electrode potentials are quoted with respect to the saturated calomel electrode (SCE). All kinetic measurements were made at  $24 \pm 0.5$  °C.

### Results and Discussion

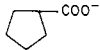
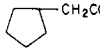
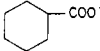
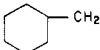
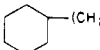
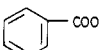
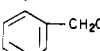
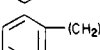
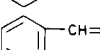
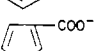
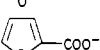
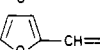
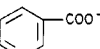
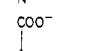
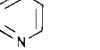
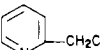
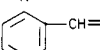
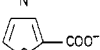
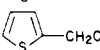
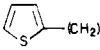
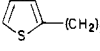
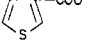
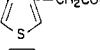
**Apparent Electrochemical Reactivities in Aqueous Media.** Table I contains electrochemical rate constants,  $k_{\text{ob}}$  ( $\text{cm s}^{-1}$ ), and transfer coefficients,  $\alpha_{\text{ob}}$  [ $=-(RT/F)(d \ln k_{\text{ob}}/dE)$ ], for the one-electron reduction of 33  $\text{Co}(\text{NH}_3)_5\text{L}^{2+}$  complexes (L = carboxylate) at mercury and gold electrodes in contact with aqueous 0.1 M  $\text{NaClO}_4$ . A common electrode potential, -100 mV, is chosen so to facilitate intercomparison, of the data; this value minimized the extent of  $\ln k_{\text{ob}}-E$  data extrapolation. In any case, the relative rate constants are not greatly dependent on the electrode potential since the values of  $\alpha_{\text{ob}}$  lie mostly in the range ca. 0.65-0.8 (Table I). Most rate measurements were made in solutions acidified to pH 2-3 with  $\text{HClO}_4$ . Only small or negligible (2-fold or less) differences in the values of  $k_{\text{ob}}$  were obtained when neutral media were used instead, even though several of the Co(III) complexes (in particular the nitrogen heterocycles<sup>9</sup>) are sufficiently strongly basic to be protonated even at pH 3. (For these systems,  $k_{\text{ob}}$  is slightly up to 1.5-2-fold larger in neutral media.)

All the Co(III) complexes were electroreduced in a single-electron step, at least at potentials on the rising part of the polarographic or voltammetric waves, ca. +100 to -300 mV, where the electrochemical kinetics could be obtained. Thus, a well-defined diffusion-controlled current plateau was obtained in each case, corresponding to one-electron reduction with diffusion coefficients in the range  $7 (\pm 2) \times 10^{-6} \text{ cm}^2 \text{ s}^{-1}$ . This also indicates that the carboxylate ligands are not reduced under these conditions, in either coordinated or free form since they are released upon formation of Co(II). Indeed, solutions containing the free ligands exhibited no electroreduction until potentials markedly more negative of -300 mV.

- (3) (a) Vlcek, A. A. *Proc. 6th Int. Conf. Coord. Chem.* **1961**, 590. (b) Endicott, J. F.; Taube, H. *J. Am. Chem. Soc.* **1964**, *86*, 1686. (c) Satterberg, T. L.; Weaver, M. J. *J. Phys. Chem.* **1978**, *82*, 1784.  
 (4) Marcus, R. A. *J. Phys. Chem.* **1963**, *67*, 853.  
 (5) (a) Li, T. T.-T.; Weaver, M. J. *J. Am. Chem. Soc.* **1984**, *106*, 6106. (b) Li, T. T.-T.; Weaver, M. J. *J. Electroanal. Chem. Interfacial Electrochem.*, in press. (c) Li, T. T.-T.; Weaver, M. J. in preparation.  
 (6) For example, see: (a) Taube, H.; Gould, E. S. *Acc. Chem. Res.* **1969**, *2*, 321. (b) Fan, F.-R. F.; Gould, E. S. *Inorg. Chem.* **1974**, *13*, 2639.

- (7) Dockal, E. R.; Everhart, E. T.; Gould, E. S. *J. Am. Chem. Soc.* **1971**, *93*, 5661.  
 (8) Tadayoni, M. A.; Weaver, M. J. *J. Electroanal. Chem. Interfacial Electrochem.*, in press.  
 (9) For example: Thamburaj, P. K.; Loar, M. K.; Gould, E. S. *Inorg. Chem.* **1977**, *16*, 1946.

**Table I.** Rate Parameters for Reduction of  $\text{Co}(\text{NH}_3)_5\text{L}^{2+}$  Complexes at Mercury- and Gold-Aqueous Interfaces at  $-100$  mV vs. SCE and by  $\text{Ru}(\text{NH}_3)_6^{2+}$  in Aqueous Solution

system no.	ligand L	mercury electrode		gold electrode		$\text{Ru}(\text{NH}_3)_6^{2+}$ $k_h^c$ , $\text{M}^{-1} \text{s}^{-1}$
		$k_{\text{ob}}^a$ , $\text{cm s}^{-1}$	$\alpha_{\text{ob}}^b$	$k_{\text{ob}}^a$ , $\text{cm s}^{-1}$	$\alpha_{\text{ob}}^b$	
1	$\text{CH}_3\text{COO}^-$	$8.5 \times 10^{-4}$	0.58	$3.1 \times 10^{-5}$	0.70	$1.8 \times 10^{-2}$
2	$\text{HCOO}^-$	$3.2 \times 10^{-3}$	0.52	$6.5 \times 10^{-5}$	0.71	$8.2 \times 10^{-2}$
3	$\text{CCl}_3\text{COO}^-$	$4.2 \times 10^{-2}$	0.46	$6.8 \times 10^{-3}$	0.73	$2.5 \times 10^{-1}$
4	$\text{CF}_3\text{COO}^-$	$6.5 \times 10^{-3}$	0.55	$3.2 \times 10^{-4}$	0.67	$1.8 \times 10^{-1}$
5	$(\text{CH}_3)_3\text{COO}^-$	$4.0 \times 10^{-3}$	0.57	$3.0 \times 10^{-5}$	0.66	$8.7 \times 10^{-3}$
6	$\text{CH}_3\text{C}(\text{O})\text{COO}^-$	$4.0 \times 10^{-3}$	0.51	$1.2 \times 10^{-4}$	0.52	$1.2 \times 10^{-1}$
7	$\text{HC}(\text{O})\text{COO}^-$	$1.5 \times 10^{-3}$	0.50	$1.0 \times 10^{-4}$	0.52	$5.9 \times 10^{-2}$
8	$\text{CH}_2\text{OHCOO}^-$	$2.4 \times 10^{-3}$	0.47	$4.8 \times 10^{-5}$	0.66	$4.7 \times 10^{-2}$
9	$\text{CH}_3\text{C}(\text{OH})\text{HCOO}^-$	$1.1 \times 10^{-3}$	0.50	$6.0 \times 10^{-5}$	0.72	$4.7 \times 10^{-2}$
10	$\text{CH}_2\text{FCOO}^-$	$2.0 \times 10^{-3}$	0.52	$1.8 \times 10^{-4}$	0.70	$1.1 \times 10^{-1}$
11		$1.1 \times 10^{-2}$	0.52	$4.5 \times 10^{-4}$	0.77	$1.2 \times 10^{-2}$
12		$2.5 \times 10^{-2}$	0.57	$5.0 \times 10^{-4}$	0.77	$1.3 \times 10^{-2}$
13		$8.5 \times 10^{-3}$	0.52	$4.6 \times 10^{-4}$	0.77	$1.8 \times 10^{-2}$
14		$2.0 \times 10^{-2}$	0.51	$1.6 \times 10^{-3}$	0.74	$4.6 \times 10^{-2}$
15		$6.1 \times 10^{-2}$	0.50	$3.1 \times 10^{-3}$	0.70	$3.3 \times 10^{-2}$
16		$1.0 \times 10^{-2}$	0.50	$1.2 \times 10^{-2}$	0.65	$1.7 \times 10^{-2}$
17		$1.1 \times 10^{-2}$	0.55	$6.5 \times 10^{-3}$	0.66	$5.1 \times 10^{-2}$
18		$8.7 \times 10^{-2}$	0.51	$9.7 \times 10^{-3}$	0.64	$2.8 \times 10^{-2}$
19		$1.2 \times 10^{-2}$	0.51	$2.0 \times 10^{-2}$	0.56	$4.2 \times 10^{-2}$
20		$7.4 \times 10^{-3}$	0.61	$1.1 \times 10^{-3}$	0.83	$1.2 \times 10^{-2}$
21		$8.3 \times 10^{-3}$	0.55	$1.5 \times 10^{-3}$	0.86	$1.9 \times 10^{-2}$
22		$2.1 \times 10^{-3}$	0.51	$1.6 \times 10^{-3}$	0.53	$1.9 \times 10^{-2}$
23		$1.4 \times 10^{-2}$	0.56	$1.5 \times 10^{-3}$	0.86	$1.4 \times 10^{-2}$
24		$1.0 \times 10^{-2}$	0.53	$1.3 \times 10^{-3}$	0.85	$1.3 \times 10^{-2}$
25		$8.0 \times 10^{-3}$	0.51	$8.9 \times 10^{-3}$	0.80	$1.5 \times 10^{-2}$
26		$1.9 \times 10^{-2}$	0.53	$7.2 \times 10^{-3}$	0.87	$1.0 \times 10^{-2}$
27		$5.0 \times 10^{-3}$	0.75	$2.3 \times 10^{-2}$	0.71	$1.3 \times 10^{-2}$
28		$2.1 \times 10^{-3}$	0.74	$7.3 \times 10^{-3}$	0.75	$3.5 \times 10^{-2}$
29		$1.7 \times 10^{-3}$	0.65	$7.0 \times 10^{-3}$	0.65	$3.2 \times 10^{-2}$
30		$1.1 \times 10^{-3}$	0.72	$3.0 \times 10^{-3}$	0.57	$1.1 \times 10^{-2}$
31		$5.2 \times 10^{-3}$	0.76	$2.8 \times 10^{-2}$	0.72	$1.3 \times 10^{-2}$
32		$2.0 \times 10^{-3}$	0.71	$7.5 \times 10^{-3}$	0.79	$1.8 \times 10^{-2}$
33		$1.1 \times 10^{-3}$	0.69	$3.2 \times 10^{-2}$	0.62	$4.1 \times 10^{-2}$

<sup>a</sup> Observed rate constant for electroreduction of given  $\text{Co}(\text{NH}_3)_5\text{L}^{2+}$  complex at the mercury or gold electrode, as indicated, at  $-100$  mV vs. SCE in  $0.1 \text{ M NaClO}_4 + 5 \text{ mM HClO}_4$ . <sup>b</sup> Observed transfer coefficient at the mercury or gold electrode, as indicated, corresponding to listed value of  $k_{\text{ob}}$ . <sup>c</sup> Observed rate constant for homogeneous reduction of given  $\text{Co}(\text{NH}_3)_5\text{L}^{2+}$  complex by  $\text{Ru}(\text{NH}_3)_6^{2+}$  in aqueous  $0.05 \text{ M}$  sodium trifluoroacetate containing  $5\text{--}20 \text{ mM}$  trifluoroacetic acid.

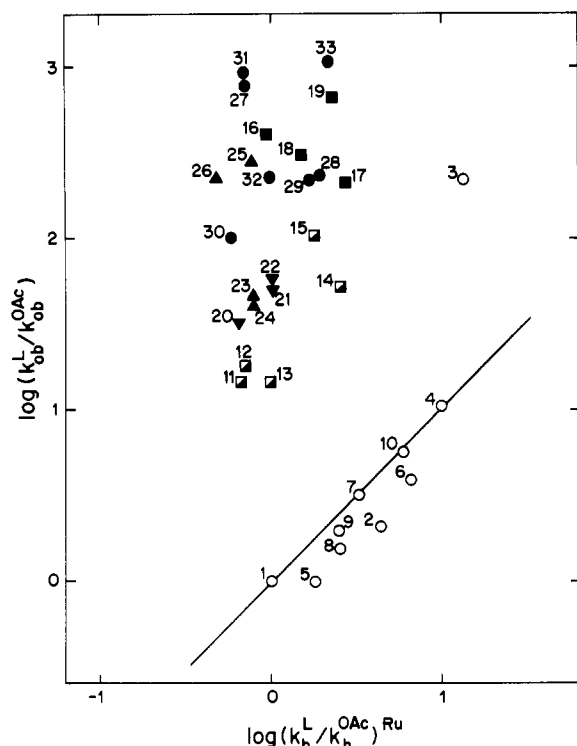


**Figure 1.** Logarithm of ratio of rate constants,  $k_{ob}^L$  ( $\text{cm s}^{-1}$ ), for electroreduction of given  $\text{Co}(\text{NH}_3)_5\text{L}^{2+}$  complex with respect to that for  $\text{Co}(\text{NH}_3)_5\text{OAc}^{2+}$ ,  $k_{ob}^{\text{OAc}}$ , at mercury in aqueous 0.1 M  $\text{NaClO}_4$  + 5 mM  $\text{HClO}_4$  at  $-100$  mV vs. SCE plotted against corresponding rate ratio,  $\log(k_h^L/k_h^{\text{OAc}})_{\text{Ru}}$ , for homogeneous second-order reduction by  $\text{Ru}(\text{NH}_3)_6^{2+}$  in aqueous 0.05 M sodium trifluoroacetate acid containing 5–20 mM trifluoroacetic acid. Kinetic data are detailed in Table I. Numbered points refer to system numbers given in Table I. Key to ligand types: (O) acyclic aliphatics; (□) aliphatic rings; (■) benzene rings; (▼) furans; (▲) pyridines; (●) thiophenes.

The various substituents on the carboxylate ligands can be categorized as follows: (i) small acyclic aliphatic groups (systems 1–10); (ii) groups containing five- or six-membered aliphatic rings (systems 11–15); (iii) groups containing benzene rings (systems 16–19); (iv) furan substituents (systems 20–22); (v) pyridine substituents (systems 23–26); (vi) thiophene substituents (systems 27–33). Of these ligands, (v) and (vi) contain heteroatoms (nitrogen and sulfur, respectively) that might be expected to bind to metal surfaces and therefore engender facile inner-sphere electroreduction pathways. The  $k_{ob}$  values for reduction of these reactants at mercury are indeed typically  $10^2$ – $10^3$ -fold larger than for those containing small aliphatic groups; this is reasonably attributed to such inner-sphere catalyses.<sup>1h</sup> However, inspection of Table I reveals that large and even comparable electrochemical reactivities are also observed for reactants containing other alicyclic and aromatic substituents, especially benzene rings, that lack such surface “lead-in” groups.

These effects are illustrated more clearly in Figure 1, which is a plot of  $\log(k_{ob}^L/k_{ob}^{\text{OAc}})$ , where  $k_{ob}^L$  and  $k_{ob}^{\text{OAc}}$  are the electrochemical rate constants for the reduction of a given complex and  $\text{Co}(\text{NH}_3)_5\text{OAc}^{2+}$ , respectively, at mercury at  $-100$  mV, against  $\log(k_h^L/k_h^{\text{OAc}})$ , where  $k_h^L$  and  $k_h^{\text{OAc}}$  are the corresponding rate constants for the homogeneous reduction by  $\text{Ru}(\text{NH}_3)_6^{2+}$ . The reduction of  $\text{Co}(\text{NH}_3)_5\text{OAc}^{2+}$  was selected as the “reference reaction” in view of the simple structure of the acetate ligand. Provided that the electrochemical, as well as homogeneous, reactions follow outer-sphere pathways, from eq 1 we expect that

$$\log(k_{ob}^L/k_{ob}^{\text{OAc}}) \approx \log(k_h^L/k_h^{\text{OAc}}) \quad (2)$$

since then the work term corrections should be similar for each

reaction and thereby cancel in the rate ratios.

Inspection of Figure 1 reveals that reactants containing acyclic aliphatic [class (i)] substituents do yield good agreement with eq 2 in that almost all the points are close to the predicted straight line shown, having unit slope and zero intercept. This suggests that these electrochemical reactions all proceed via similar, presumably outer-sphere, transition states (vide infra). However, the remaining points are uniformly above this line, so that the values of  $k_{ob}$  for all 24 reactants having ring-containing substituents [classes (ii)–(vi)] are between 20- and  $10^3$ -fold larger than are expected from the homogeneous reactivities on the basis of eq (2). Some interesting trends can nonetheless be discerned from Figure 1. Most prominently, the “degree of electrocatalysis” as measured by the vertical displacement of the experimental points above the “theoretical” solid line is systematically dependent upon the nature of the substituent ring. We shall express this electrocatalysis as the rate ratio  $k_{ob}^L/k_{ob}^{\text{eq}2}$ , where  $k_{ob}^{\text{eq}2}$  is the electrochemical rate constant corresponding to  $k_{ob}^L$  that is predicted from eq 2 (i.e., from the straight line in Figure 1). For the various substituent classes, the approximate range of values of  $k_{ob}^L/k_{ob}^{\text{eq}2}$  is as follows: alicyclic aliphatics [class (ii)], 10–30; benzene substituents [class (iii)], 100–300; furans [class (iv)], 50; nitrogen heterocyclics [class (v)], 50–300; thiophenes [class (vi)],  $10^2$ – $10^3$ . Of the class (i) substituents, only  $\text{CCl}_3\text{COO}^-$  yields a substantially higher electrochemical reactivity than predicted by eq 2 (Figure 1).

The observed electrochemical rate constants can usefully be separated into precursor-state and electron-transfer step contributions according to<sup>10</sup>

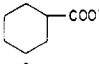
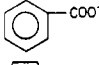
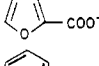
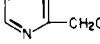
$$k_{ob} = K_p k_{et} \quad (3)$$

where  $K_p$  (cm) is the equilibrium constant for forming the precursor state (i.e., the reaction site in the double layer) from the bulk reactant and  $k_{et}$  ( $\text{s}^{-1}$ ) is the unimolecular rate constant for the elementary electron-transfer step. The dependence of  $k_{et}$  as well as  $K_p$  upon the carboxylate ligand structure has been scrutinized in detail for a number of thiophene-(carboxylato)cobalt(III) reductions occurring via thiophene-bridged transition states.<sup>1h</sup> Substantially (ca. 10–20-fold) smaller values of  $k_{et}$  are found at mercury electrodes with bridging ligands containing one or more methylenes between the thiophene surface-binding group and the cobalt compared to those for reactants with ligands featuring uninterrupted conjugation. These differences appear to be due to the occurrence of nonadiabatic pathways (i.e., where the electronic transmission coefficient  $\kappa_{el} < 1$ ) for the former systems. For the latter, it appears that  $\kappa_{el} \sim 1$ ; the reactivity enhancement,  $k_{ob}^L/k_{ob}^{\text{eq}2}$ , for these inner-sphere systems relative to structurally similar outer-sphere reactions (such as  $\text{Co}(\text{NH}_3)_5\text{OAc}^{2+}$  reduction) is due largely to the large (ca.  $10^3$ -fold) increases in  $K_p$  resulting from surface attachment.<sup>1h</sup>

Values of  $K_p$  at mercury were not determined directly for the other  $\text{Co}(\text{III})$  carboxylate reactants in Table I since they are insufficiently large ( $K_p \lesssim 10^{-4}$  cm) to be extracted reliably from rapid linear-sweep voltammetry.<sup>1h</sup> Nonetheless, broadly speaking, the variations of  $k_{ob}^L/k_{ob}^{\text{eq}2}$  with the substituent ring structure noted above can also be rationalized in terms of differences in precursor stabilities (vide infra). Thus, the presence of unsaturated rings [classes (iii)–(vi)] yields substantially larger  $k_{ob}^L/k_{ob}^{\text{eq}2}$  values than for the aliphatic rings. This suggests that ring–metal surface  $\pi$  interactions and possibly “hydrophobic interactions” contribute importantly to the stabilization of the precursor state, although differences in  $\kappa_{el}$ , and hence in  $k_{et}$ , may also play a significant role. In particular, the observation that the  $k_{ob}^L/k_{ob}^{\text{eq}2}$  values for the benzene substituents are close to those for the thiophene complexes implicates the importance of such aromatic rings to the precursor stability. The ca. 5–50-fold larger values of  $k_{ob}^L/k_{ob}^{\text{eq}2}$  for the

(10) Hupp, J. T.; Weaver, M. J. *J. Electroanal. Chem. Interfacial Electrochem.* 1983, 152, 1.

**Table II.** Unimolecular Rate Parameters for Outer-Sphere Reduction of  $\text{Co}^{\text{III}}(\text{NH}_3)_5\text{L}$  Complexes at  $-200$  mV vs. SCE at Chloride-Coated Silver–Aqueous Interface and Comparison with Corresponding Rate Parameters for Aqueous Solution Reactants at Mercury Electrodes

ligand L	$k_{\text{et}}^a$ , $\text{s}^{-1}$	$\alpha_{\text{et}}^b$	$k_{\text{et}}^{\text{cor},c}$ , $\text{s}^{-1}$	$k_{\text{ob}}^d$ , $\text{cm s}^{-1}$	$\alpha_{\text{ob}}^e$	$K_p^f$ , cm	$K_o^g$ , cm
$\text{NH}_3$	20	0.68	$4 \times 10^2$	$2.5 \times 10^{-4}$	0.7	$6 \times 10^{-7}$	$8 \times 10^{-8}$
$\text{CH}_3\text{COO}^-$	15	0.7	$3 \times 10^2$	$3.5 \times 10^{-4}$	0.7	$1.2 \times 10^{-6}$	$3 \times 10^{-7}$
	15	0.7	$3 \times 10^2$	$8 \times 10^{-3}$	0.75	$3 \times 10^{-5}$	$8 \times 10^{-6}$
	20	0.65	$4 \times 10^2$	0.15	0.65	$3.5 \times 10^{-4}$	$1 \times 10^{-4}$
	50	0.75	$1 \times 10^3$	$3.5 \times 10^{-2}$	0.8	$3.5 \times 10^{-5}$	$1 \times 10^{-5}$
	15	0.7	$3 \times 10^2$	0.2	0.8	$6.5 \times 10^{-4}$	$2 \times 10^{-4}$

<sup>a</sup> Unimolecular rate constant for electron-transfer step at  $-200$  mV, determined by means of rapid linear-sweep voltammetry for electrostatically adsorbed reactant at silver electrode in 0.1 M KCl as outlined in ref 8. <sup>b</sup> Transfer coefficient for electron-transfer step, determined as in footnote a.<sup>8</sup> <sup>c</sup> Work-corrected unimolecular rate constant at  $-200$  mV, estimated from  $k_{\text{et}}$  by correcting for potential at reaction plane at chloride-coated silver ( $\approx -110$  mV) (see text and ref 8). <sup>d</sup> Observed rate constant for solution reactant at  $-200$  mV at mercury electrodes in 0.1 M  $\text{NaClO}_4$  (pH 2.5) determined by using normal-pulse polarography. <sup>e</sup> Observed transfer coefficient for solution reactant, corresponding to  $k_{\text{ob}}$ . <sup>f</sup> Precursor stability constant at mercury–aqueous interface, determined from eq 5. <sup>g</sup> Electrostatic-corrected precursor stability constant at mercury–aqueous interface, determined from  $K_p'$  by using eq 6, with  $\phi_r = -20$  mV (see text).

thiophene reactants relative to those found with the closely analogous furan substituents (Figure 1) (i.e., where the sulfur atom is replaced by oxygen) nevertheless illustrate the influence of the heterocyclic atom upon  $K_p$ , probably as a result of surface  $\sigma$  bonding.<sup>1h</sup> Such effects also likely to be responsible for the ca. 20-fold larger value of  $k_{\text{ob}}$  for  $\text{L} = \text{CCl}_3\text{COO}^-$  with respect to  $\text{L} = \text{CF}_3\text{COO}^-$  (points 3 and 4, Figure 1), presumably associated with chlorine–mercury surface interactions.

An alternative way of examining such ligand effects upon the redox reactivities involves their correlation with inductive and steric parameters for the various substituent groups.<sup>6b,11</sup> Figure 2A is a plot of  $\log k_{\text{ob}}$  for 13  $\text{Co}(\text{NH}_3)_5\text{L}^{2+}$  electroreduction reactions against the Taft inductive parameter,  $\sigma^*$ , for each carboxylate substituent.<sup>12</sup> For the acyclic aliphatic substituents,  $\log k_{\text{ob}}$  increases approximately linearly with increasing  $\sigma^*$  (i.e., with increasing electron-withdrawal power of the organic substituent). Although the effect is relatively small, it is consistent with thermodynamic expectations since electron withdrawal from the cobalt redox center is expected to destabilize  $\text{Co}(\text{III})$  relative to  $\text{Co}(\text{II})$ , shifting the (unknown)  $\text{Co}(\text{III})/\text{Co}(\text{II})$  formal potential positive and thereby increasing  $k_{\text{ob}}$  at a given electrode potential. A similar correlation is seen for the corresponding homogeneous reactivities,  $\log k_{\text{h}}$ , of  $\text{Co}(\text{NH}_3)_5\text{L}^{2+}$  with  $\text{Ru}(\text{NH}_3)_6^{2+}$  in Figure 2B, even though some systems, for example  $\text{L} = (\text{CH}_3)_3\text{COO}^-$ , have  $k_{\text{h}}$  values that are somewhat smaller than expected. This may be due to the influence of steric effects associated with the electrostatically preferred approach of the  $\text{Ru}(\text{NH}_3)_6^{2+}$  reductant to the negatively charged carboxylate ligand. This effect is, however, probably small for most systems in Figure 2B since addition of a suitably weighted term based on the Taft steric parameter<sup>12</sup> does little to improve the correlation.

While a consistent  $\log k_{\text{h}}-\sigma^*$  correlation is also observed for reactants with ring-containing as well as acyclic substituents (Figure 2B), the former yields electrochemical reactivities that are substantially larger than expected from the  $\log k_{\text{ob}}-\sigma^*$  correlation (Figure 2A). This provides further evidence that the unexpectedly large values of  $k_{\text{ob}}$  for alicyclic as well as aromatic substituents (Figure 1) arise from the influence of the interfacial environment.

**Unimolecular Electrochemical Reactivities.** An additional means of examining the electrochemical reactivities of  $\text{Co}(\text{NH}_3)_5\text{L}^{2+}$  complexes involves the direct evaluation of unimolecular rate constants,  $k_{\text{et}}$ , by means of rapid linear-sweep voltammetry of

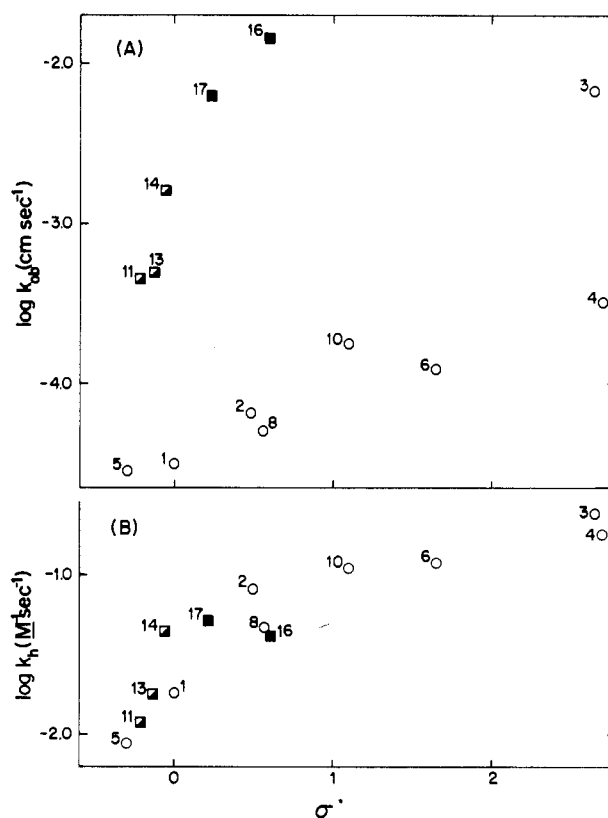


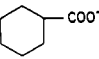
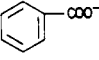
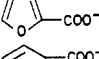
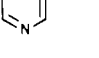
**Figure 2.** Logarithm of rate constants for (A) electroreduction of  $\text{Co}(\text{NH}_3)_5\text{L}^{2+}$  complexes at mercury and (B) homogeneous reduction by  $\text{Ru}(\text{NH}_3)_6^{2+}$  in aqueous solution plotted against the Taft inductive parameter.<sup>12</sup> For key to system numbers see Table I, and for conditions and key to symbols see footnotes to Figure 1.

electrostatically adsorbed reactant at halide-coated silver surfaces.<sup>8</sup> Table II contains values of  $k_{\text{et}}$  determined in this manner at chloride-coated silver for the reduction of five  $\text{Co}(\text{NH}_3)_5\text{L}^{2+}$  complexes and also  $\text{Co}(\text{NH}_3)_6^{3+}$  at  $-200$  mV vs. SCE. Full details of such measurements are given in ref 8. The striking feature of the  $k_{\text{et}}$  values in Table II is that, similar to the corresponding  $k_{\text{h}}$  values (Table I), they are virtually independent of the carboxylate ligand.

Such  $k_{\text{et}}$  values can also be employed to extract precursor stability constants,  $K_p$ , from the corresponding  $k_{\text{ob}}$  values obtained at the mercury–aqueous interface by using eq 3. It is preferable, however, to correct  $k_{\text{et}}$  for the double-layer potential drop,  $\phi_r$ , at the silver surface, yielding a “work-corrected” value,  $k_{\text{et}}^{\text{cor}}$ , that

- (11) (a) Barrett, M. B.; Swinehart, J. H.; Taube, H. *Inorg. Chem.* **1971**, *10*, 1983. (b) Fan F.-R. F.; Gould, E. S. *Inorg. Chem.* **1974**, *13*, 2647.  
 (12) Taft, R. W., Jr. In “Steric Effects in Organic Chemistry”; Newman, M. S., Ed.; Wiley: New York, 1956, Chapter 13. Also see: Shorter, J. In “Advances in Linear Free Energy Relationships”; Chapman, N. B., Shorter, J., Eds.; Plenum Press: New York, 1972; Chapter 2.

**Table III.** Relative Electrochemical Reactivities,  $k_{ob}^L/k_{ob}^{OAc}$ ,<sup>a</sup> and Transfer Coefficients,  $\alpha_{ob}$ ,<sup>b</sup> for Reduction of  $\text{Co}(\text{NH}_3)_5\text{L}$  Complexes at Mercury Electrodes in Various Solvents

system <sup>c</sup> no.	ligand L	$\sigma^* d$	water		propylene carbonate		formamide		DMF		Me <sub>2</sub> SO	
			$k_{ob}/k_{ob}^{OAc}$	$\alpha_{ob}$	$k_{ob}/k_{ob}^{OAc}$	$\alpha_{ob}$	$k_{ob}/k_{ob}^{OAc}$	$\alpha_{ob}$	$k_{ob}/k_{ob}^{OAc}$	$\alpha_{ob}$	$k_{ob}/k_{ob}^{OAc}$	$\alpha_{ob}$
1	$\text{CH}_3\text{COO}^-$	0	$(3.1 \times 10^{-5};$ -100 mV)	0.70	$(1.6 \times 10^{-3};$ -200 mV)	0.49	$(1.3 \times 10^{-3};$ -500 mV)	0.74	$(4.4 \times 10^{-3};$ -500 mV)	0.56	$(5 \times 10^{-3};$ -500 mV)	0.52
13		-0.15	15	0.77	0.6	0.49	2.7	0.68	2.7	0.61	0.22	0.50
16		+0.6	$4 \times 10^2$	0.65	2.4	0.53	7.7	0.65	2.5	0.66	2.0	0.51
21			50	0.86	3.1	0.49	5.5	0.68	1.4	0.61	1.5	0.54
23			50	0.85	2.4	0.47	11.5	0.65	2.6	0.57	2.2	0.50

<sup>a</sup> Electrochemical rate constant for reduction of given  $\text{Co}(\text{NH}_3)_5\text{L}^{2+}$  complex,  $k_{ob}^L$ , with respect to that for  $\text{Co}(\text{NH}_3)_5\text{OAc}^{2+}$ ,  $k_{ob}^{OAc}$ , at a given electrode potential, measured in 0.1 M tetraethylammonium perchlorate (TEAP) in nonaqueous media and in 0.1 M  $\text{NaClO}_4$  in aqueous solution. Value of  $k_{ob}^{OAc}$  ( $\text{cm s}^{-1}$ ) in each solvent, together with electrode potential (mV vs. aqueous SCE) at which it is measured, given in parentheses in first row. <sup>b</sup> Measured in same electrolytes as those noted for  $k_{ob}^L$  in footnote a. <sup>c</sup> System numbers as in Table I. <sup>d</sup> Taft inductive parameter for given carboxylate substituent, from ref 12.

would be observed at a given electrode potential if  $\phi_r = 0$ . (This value of  $k_{et}^{cor}$  can therefore be assumed to be roughly independent of the surface environment and, therefore, appropriate for mercury as well as silver surfaces.<sup>8</sup>) These quantities are related by<sup>8</sup>

$$k_{et}^{cor} = k_{et} \exp(-\alpha_{cor} F \phi_r / RT) \quad (4)$$

where the work-corrected transfer coefficient is approximated<sup>8</sup> by  $\alpha_{et} [= -(RT/F)(d \ln k_{et}/dE)]$  (Table II). For the present conditions,  $\phi_r \approx -110$  mV,<sup>8</sup> the values of  $k_{et}^{cor}$  at -200 mV obtained from  $k_{et}$  by using eq 4 are also listed in Table II. These are combined with the corresponding  $k_{ob}$  values obtained at mercury electrodes at -200 mV to yield the "effective" precursor stability constants,  $K_p'$ , given in Table II by using

$$K_p' = k_{ob} / k_{et}^{cor} \quad (5)$$

[These precursor stability constants,  $K_p'$ , differ slightly from the values,  $K_p$ , defined by eq 3 in that the former contain an electrostatic component appropriate to the effective transition-state charge ( $Z_r - \alpha_{cor}$ ), rather than to the reactant charge  $Z_r$ .<sup>13</sup>] It is useful to define a "nonelectrostatic" (or "statistical"<sup>10</sup>) component of  $K_p'$ ,  $K_o$ , given by

$$K_o = K_p' \exp[(Z_r - \alpha_{cor}) F \phi_r / RT] \quad (6)$$

where  $\phi_r$  is now the reaction-site potential at the mercury-aqueous interface. The resulting estimates of  $K_o$  for the reactions at the mercury-aqueous 0.1 M  $\text{NaClO}_4$  interface at -200 mV, assuming that  $\phi_r \approx -20$  mV under these conditions,<sup>14</sup> are listed in Table II.

For outer-sphere reactions, it is expected that<sup>15</sup>

$$K_o = \chi + (\sim 5 \times 10^{-9} \text{ cm}) \quad (7)$$

where  $\chi$  is the distance beyond the plane of closest approach over which reaction adiabaticity is retained (i.e., for which the electronic transmission coefficient,  $\kappa_{el}$ , remains close to unity). The estimates of  $K_o$  for  $\text{Co}(\text{NH}_3)_6^{3+}$  and  $\text{Co}(\text{NH}_3)_5\text{OAc}^{2+}$  reduction in Table I, ca.  $10^{-7}$  cm, are somewhat larger than that expected from eq 7,  $K_o \sim 10^{-8}$  cm, given that we anticipate that  $\chi \lesssim 1 \times 10^{-8}$  cm.<sup>15</sup> This may be due to the inevitable uncertainties contained in the above analysis or, more likely, to a nonelectrostatic contribution

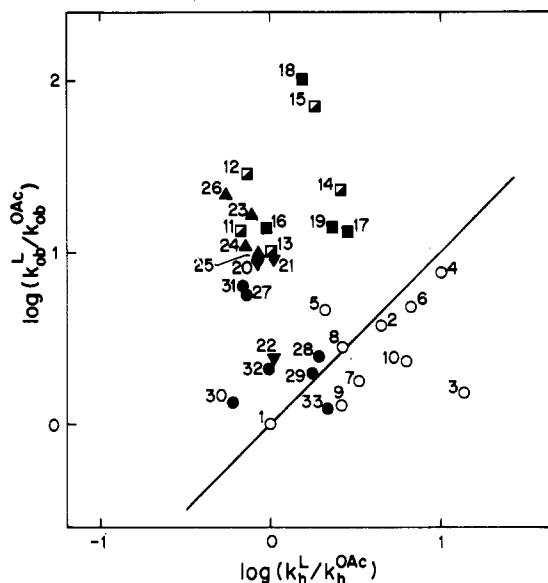


**Figure 3.** As Figure 1, but for electrochemical rate constants at the gold-aqueous interface.

to  $K_o$ . However, the estimates of  $K_o$  for the ring-containing carboxylates in Table I are substantially (ca.  $10^3$ - $10^4$ -fold) larger than expected from eq 7, again implicating the presence of strong reactant adsorption arising from "specific" interactions between the substituent ring and the metal surface.

We have also observed facile electron mediation for  $\text{Co}(\text{III})$  reduction by nitrogen heterocyclic ligands at mercury-, gold-, and platinum-aqueous interfaces.<sup>1d</sup> These effects were similarly attributed to enhancement of the precursor stability via "hydrophobic" ring-surface interactions or  $\pi$  bonding. The present systems also display such behavior at the gold-aqueous interface. A plot of  $\log(k_{ob}^L/k_{ob}^{OAc})$  at gold vs.  $\log(k_h^L/k_h^{OAc})$ , similar to that shown for mercury electrodes in Figure 1, is given in Figure 3. Although a number of systems in the latter plot display considerably more scatter than in the former, the same general trends are observed in that most of the ring-containing reactants yield markedly enhanced reactivities compared with those predicted from eq 2. One apparent anomaly is that several of the thiophene-containing reactants display  $k_{ob}$  values that are not far from this prediction (i.e., close to the straight line shown), even though these reactants are very strongly adsorbed at gold.<sup>1h</sup> This behavior is probably due to the occurrence of inhibited inner-sphere, or even outer-sphere, pathways under the dc voltammetric conditions where  $k_{ob}$  is measured, arising from blockage of the

(13) This is because  $k_{ob}$  is related to the corresponding "electrostatic work-corrected" rate constant,  $k_{cor}$ , at a given electrode potential by<sup>14</sup>  $\ln k_{ob} = \ln k_{cor} - (Z_r - \alpha_{cor}) F \phi_r / RT$ ; i.e., the work term correction is that appropriate to the effective transition-state charge ( $Z_r - \alpha_{cor}$ ) rather than  $Z_r$ . The corresponding relation between  $K_o$  and  $K_p$  [cf. eq 6] is<sup>8,10</sup>  $K_o = K_p \exp(Z_r F \phi_r / RT)$ .

(14) Weaver, M. J. *J. Electroanal. Chem. Interfacial Electrochem.* **1978**, *93*, 231.

(15) Hupp, J. T.; Weaver, M. J. *J. Phys. Chem.* **1984**, *88*, 1463.

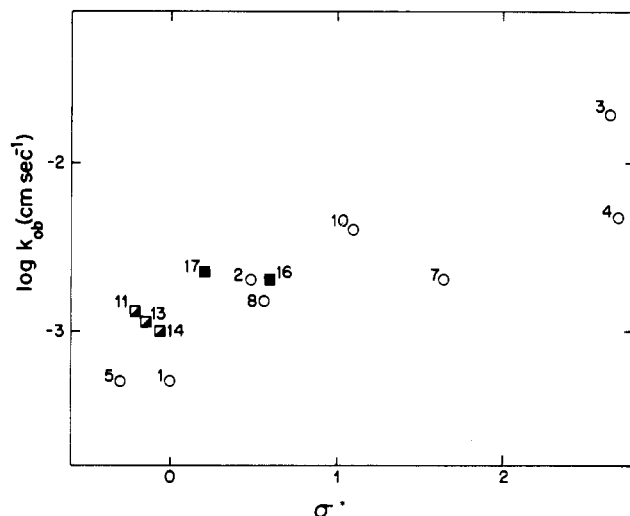


**Figure 4.** Logarithm of rate constants for electroreduction of  $\text{Co}(\text{NH}_3)_5\text{L}^{2+}$  complexes at the mercury-dimethyl sulfoxide interface at  $-500$  mV vs. SCE with  $0.1$  M tetraethylammonium perchlorate supporting electrolyte, plotted against the Taft substituent parameter. See Table I for key to system numbers and footnotes to Figure 1 for key to symbols.

electrode surface by irreversibly adsorbed reactant and the uncoordinated ligand product.

**Electrochemical Kinetics in Nonaqueous Media.** The foregoing demonstrates that strikingly large specific ligand effects can be induced on the electrochemical kinetics of even ostensibly outer-sphere reactions in aqueous solution. Inasmuch as reactant-solvent (and/or solvent-surface) interactions might be expected to play an important role, it is of interest to examine the corresponding ligand effects in nonaqueous media. Table III summarizes the electrochemical rate constants for reduction of four representative  $\text{Co}(\text{NH}_3)_5\text{L}^{2+}$  complexes with respect to that for  $\text{Co}(\text{NH}_3)_5\text{OAc}^{2+}$  reduction at mercury,  $k_{ob}^L/k_{ob}^{\text{OAc}}$ , at a given electrode potential in four nonaqueous solvents as well as in aqueous solution. The electrode potentials for each solvent was chosen so to avoid data extrapolation. The electrolyte selected for the nonaqueous kinetic measurements was  $0.1$  M tetraethylammonium perchlorate (TEAP). (The values of  $k_{ob}^L/k_{ob}^{\text{OAc}}$  were insensitive to the particular electrolyte chosen, as expected since the electrostatic work term embodied in eq 6 should be approximately the same for each reactant.)

The striking feature of the data in Table III is that the unexpectedly large values of  $k_{ob}^L/k_{ob}^{\text{OAc}}$  for ring-containing substituents seen in aqueous solution are substantially diminished in nonaqueous media, especially in propylene carbonate, DMF, and  $\text{Me}_2\text{SO}$  within which hydrogen bonding is absent. Indeed, the values of  $\log(k_{ob}^L/k_{ob}^{\text{OAc}})$  in these solvents correlate approximately with  $\sigma^*$ . This point is illustrated in Figure 4, which is a plot of  $\log k_{ob}$  vs.  $\sigma^*$  for 13 acyclic aliphatic and ring-containing reactants at the mercury- $\text{Me}_2\text{SO}$  interface. In contrast to the corresponding plot for the mercury-aqueous interface (Figure 2A) a unified correlation is obtained in Figure 4 for all the reactions irrespective of the carboxylate substituent.

This strongly suggests that these aprotic solvents, in contrast to aqueous solution, engender "normal" outer-sphere pathways for electroreduction of  $\text{Co}(\text{NH}_3)_5\text{L}^{2+}$ , at least where L lacks a strong surface-binding group. This propensity for outer-sphere behavior in these aprotic media has also been seen for  $\text{Co}(\text{en})_3^{3+/2+}$  electrochemical exchange (en = ethylenediamine), whereas unexpectedly large standard rate constants were observed at the mercury-aqueous interface.<sup>16</sup> The latter behavior also can be traced to a markedly enhanced value of  $K_o$ .<sup>8</sup> Especially in the strongly "electron-donating" solvents  $\text{Me}_2\text{SO}$  and DMF, the observed behavior can be understood in terms of the strong reactant

solvation arising from specific ligand-solvent interactions involving the ammine hydrogens. These interactions exert important influences upon the redox thermodynamics.<sup>17</sup> Presumably, such strong solvation will hinder the close approach of the reactant to the metal surface. "Hydrophobic" interactions<sup>18</sup> between the organic substituents and the surface, which probably aid reactant adsorption in aqueous solution, will be absent in aprotic media. (Indeed, the strong adsorption of a variety of organic molecules seen at metal-aqueous interfaces<sup>19</sup> is largely absent for aprotic solvents.)

The presence of "abnormal" electroreduction pathways in aqueous solution is also suggested by the larger values of  $\alpha_{ob}$  seen under these conditions compared to those in nonaqueous media (Tables I and III). Although complicated by diffuse-layer effects,<sup>14</sup> these values are suggestive of reaction sites closer to the electrode surface, as would be anticipated for reaction pathways featuring specific reactant-electrode interactions.

**Concluding Remarks.** The present results add substantially to the growing body of evidence indicating that substantial deviations from normal outer-sphere pathways often occur for mechanistically simple electrochemical reactions involving metal complexes in aqueous solution even when the coordinated ligands lack surface-binding groups.<sup>14,2d,8,16</sup> These "surface environmental" effects can be very large, yielding up to ca.  $10^4$ -fold alterations in  $k_{ob}$ . Broadly speaking, they are attributable primarily to variations in the precursor stability associated either with specific ligand-surface interactions or with differences between the reactant-solvent interactions in the bulk solution and at the reaction site.<sup>1d</sup> As noted in ref 1d, one key difference between electrodes and homogeneous redox reagents is that the former always offer the possibility of delocalized reactant-surface interactions for reactants containing extended organic structural units.

Precursor structures involving  $\pi$  interactions between substituent rings and the reductant have been postulated to occur for homogeneous reactions related to those considered here in order to explain unexpectedly large reactivities.<sup>20</sup> Another mechanism commonly proposed to account for enhanced homogeneous reduction rates involves sequential reduction of the organic ligand and the metal redox center.<sup>21</sup> Similar pathways could also account for some enhanced electrochemical reaction rates with reactants containing reducible ligand. However, the impetus for such two-step pathways in competition with the alternative one-step mechanism presumably includes a diminution of the effective reorganization energy since the latter, but not the former, process necessarily involves simultaneous activation of both oxidizing and reducing redox centers. The electrochemical reductions, on the other hand, only involve reorganization of the oxidizing center since the metal surface "reductant" does not require nuclear activation. In any case, such ligand-reduction pathways cannot account for the present results since as noted above the organic carboxylate ligands employed here do not undergo electroreduction in the potential range where the  $\text{Co}(\text{III})$  reduction kinetics are monitored.

Nevertheless, the available evidence indicates that organic ligand effects upon electrochemical reactivities can be as striking as, if somewhat different from, those observed for homogeneous redox processes. The further quantitative delineation of such effects, especially with parallel measurements of reactant adsorption, would be extremely worthwhile.

**Acknowledgment.** A number of initial experiments were performed by Drs. S. Srinivasan and S. Barr. This work is supported by the Air Force Office of Scientific Research and the Office of

(16) Farmer, J. K.; Gennett, T.; Weaver, M. J. *J. Electroanal. Chem. Interfacial Electrochem.*, in press.

(17) Sahami, S.; Weaver, M. J. *J. Electroanal. Chem. Interfacial Electrochem.* **1981**, *122*, 171.

(18) Franks, F. In "Water - A Comprehensive Treatise"; Franks, F., Ed.; Plenum Press: New York, 1975, Vol. 4, Chapter 1.

(19) For example: Damaskin, B. B.; Petrii, O. A.; Batrakov, V. V. "Adsorption of Organic Compounds on Electrodes"; Plenum Press: New York, 1971.

(20) Radlowski, C. A.; Gould, E. S. *Inorg. Chem.* **1979**, *18*, 1289. Srinivasan, V. S.; Radlowski, C. A.; Gould, E. S. *Inorg. Chem.* **1981**, *20*, 2094.

(21) For example: Heh, J. C.-K.; Gould, E. S. *Inorg. Chem.* **1978**, *17*, 3138.



Naval Research. M.J.W. acknowledges a fellowship from the Alfred P. Sloan Foundation.

**Registry No.** Co(NH<sub>3</sub>)<sub>5</sub>OAc<sup>2+</sup>, 16632-78-3; Co(NH<sub>3</sub>)<sub>6</sub>, 14695-95-5; Ru(NH<sub>3</sub>)<sub>6</sub><sup>2+</sup>, 19052-44-9; Co(NH<sub>3</sub>)<sub>5</sub>(HCOO)<sup>2+</sup>, 19173-64-9; Co(NH<sub>3</sub>)<sub>5</sub>(CCl<sub>3</sub>COO)<sup>2+</sup>, 19998-53-9; Co(NH<sub>3</sub>)<sub>5</sub>(CF<sub>3</sub>COO)<sup>2+</sup>, 19173-66-1; Co(NH<sub>3</sub>)<sub>5</sub>((CH<sub>3</sub>)<sub>2</sub>CCOO)<sup>2+</sup>, 33887-25-1; Co(NH<sub>3</sub>)<sub>5</sub>(CH<sub>3</sub>C(O)COO)<sup>2+</sup>, 19306-91-3; Co(NH<sub>3</sub>)<sub>5</sub>(HC(O)COO)<sup>2+</sup>, 19306-90-2; Co(NH<sub>3</sub>)<sub>5</sub>-(CH<sub>2</sub>OHCOO)<sup>2+</sup>, 31279-86-4; Co(NH<sub>3</sub>)<sub>5</sub>(CH<sub>3</sub>C(OH)HCOO)<sup>2+</sup>, 34464-03-4; Co(NH<sub>3</sub>)<sub>5</sub>(CH<sub>2</sub>FCOO)<sup>2+</sup>, 51965-33-4; Co(NH<sub>3</sub>)<sub>5</sub>L<sup>2+</sup> (L = cyclopentylcarboxylato), 51965-54-9; Co(NH<sub>3</sub>)<sub>5</sub>L<sup>2+</sup> (L = (cyclopentylmethyl)carboxylato), 96041-24-6; Co(NH<sub>3</sub>)<sub>5</sub>L<sup>2+</sup> (L = cyclohexylmethylcarboxylato), 52593-65-4; Co(NH<sub>3</sub>)<sub>5</sub>L<sup>2+</sup> (L = (cyclohexylmethyl)carboxylato), 51965-55-0; Co(NH<sub>3</sub>)<sub>5</sub>L<sup>2+</sup> (L = (cyclohexylethyl)carboxylato), 96041-25-7; Co(NH<sub>3</sub>)<sub>5</sub>L<sup>2+</sup> (L = benzoato), 30931-77-2;

Co(NH<sub>3</sub>)<sub>5</sub>L<sup>2+</sup> (L = benzeneacetato), 40544-43-2; Co(NH<sub>3</sub>)<sub>5</sub>L<sup>2+</sup> (L = benzenepropanato), 96041-26-8; Co(NH<sub>3</sub>)<sub>5</sub>L<sup>2+</sup> (L = benzenepropenato), 96148-95-7; Co(NH<sub>3</sub>)<sub>5</sub>L<sup>2+</sup> (L = furan-3-carboxylato), 88563-81-9; Co(NH<sub>3</sub>)<sub>5</sub>L<sup>2+</sup> (L = furan-2-carboxylato), 52021-51-9; Co(NH<sub>3</sub>)<sub>5</sub>L<sup>2+</sup> (L = pyridine-3-carboxylato), 52021-52-0; Co(NH<sub>3</sub>)<sub>5</sub>L<sup>2+</sup> (L = pyridine-4-carboxylato), 58846-54-1; Co(NH<sub>3</sub>)<sub>5</sub>L<sup>2+</sup> (L = pyridine-2-acetato), 62816-16-4; Co(NH<sub>3</sub>)<sub>5</sub>L<sup>2+</sup> (L = pyridine-3-propenato), 46840-94-2; Co(NH<sub>3</sub>)<sub>5</sub>L<sup>2+</sup> (L = thiophene-2-carboxylato), 55835-99-9; Co(NH<sub>3</sub>)<sub>5</sub>L<sup>2+</sup> (L = thiophene-2-acetato), 88563-74-0; Co(NH<sub>3</sub>)<sub>5</sub>L<sup>2+</sup> (L = thiophene-2-propenato), 88563-75-1; Co(NH<sub>3</sub>)<sub>5</sub>L<sup>2+</sup> (L = thiophene-2-butanato), 88563-76-2; Co(NH<sub>3</sub>)<sub>5</sub>L<sup>2+</sup> (L = thiophene-3-carboxylato), 88563-77-3; Co(NH<sub>3</sub>)<sub>5</sub>L<sup>2+</sup> (L = thiophene-3-acetato), 88563-78-4; Co(NH<sub>3</sub>)<sub>5</sub>L<sup>2+</sup> (L = thiophene-2-propenato), 88642-97-1; Ag, 7440-22-4; Au, 7440-57-5; Hg, 7439-97-6; Cl<sup>-</sup>, 16887-00-6.

Contribution from the Laboratoire de Spectrochimie des Eléments de Transition, ERA 672, Université de Paris-Sud, 91405 Orsay, France, and Department of Chemistry, Oregon State University, Corvallis, Oregon 97331

## Magnetic, EPR, and Mössbauer Properties of an $S = 3/2$ Ground State Heterotrinary Cluster Containing One Iron(III) and Two Copper(II) Ions

IRÈNE MORGENSTERN-BADARAU\*<sup>1a</sup> and H. HOLLIS WICKMAN<sup>1b</sup>

Received August 3, 1984

Magnetic susceptibility data and EPR and Mössbauer spectra are reported that are attributed to formation of the heterotrinary cluster  $[[\text{Cu}(\text{Mesalen})]_2\text{Fe}(\text{acac})](\text{NO}_3)_2$  (MesalenH<sub>2</sub> = *N,N'*-bis(methylsalicylaldehyde) ethylenediimine; acac = acetylacetonato). The material has not yet been isolated in crystalline form suitable for X-ray structure analysis. The magnetic data have been used to deduce the indicated structure. The Cu(II) ions are equally coupled antiferromagnetically ( $J_{\text{Cu-Fe}} = -63 \text{ cm}^{-1}$ ,  $g = 2.08$ ) to the Fe(III) ion but are only weakly coupled ( $J_{\text{Cu-Cu}} = 0$ ) to each other. The resulting  $S = 3/2$  coupled ground state is split by crystal field interactions described by a positive  $D$  term ( $D = 7.2 \text{ cm}^{-1}$ ). Only the ground doublet is EPR active, with  $g$  factors of 4.68, 3.26, and 1.96. The Mössbauer spectra at all temperatures are relaxation broadened; hence, accurate assignment of hyperfine parameters could not be made. The data for the helium temperature range show spectra consistent with an effective relaxation rate that increases as temperature is lowered. This arises from depopulation of the excited, slowly relaxing Kramers doublet with concomitant population of the more rapidly relaxing, EPR active, ground doublet.

### Introduction

The magnetism of transition-metal cluster complexes is often dominated by intracluster exchange interactions that reflect important chemical bonds involving the metal atoms. Many homobinuclear and homopolynuclear metal complexes are known that display interesting magnetic properties dependent upon such exchange interactions. By contrast, the literature regarding heterobinuclear and heteropolynuclear metal clusters is much less extensive. One area of current interest involves Cu(II)-Fe(III) heterodimers, which are potential analogue compounds for a redox center of the cytochrome oxidase molecule.<sup>2-4</sup> These systems also raise important magnetochemical questions in which the focus is more upon the fundamental electronic properties of the compound.<sup>5,6</sup> In this context, we report here evidence for what appears to be the first example of a heterotrinary cluster containing two Cu(II) ions and one Fe(III) ion. As shown below these ions are in the present case antiferromagnetically coupled to an  $S = 3/2$  ground state. The complex,  $[[\text{Cu}(\text{Mesalen})]_2\text{Fe}(\text{acac})](\text{NO}_3)_2$ , noted as  $[\text{2Cu-Fe}]$  (MesalenH<sub>2</sub> = *N,N'*-bis(methylsalicylaldehyde) ethylenediimine; acac = acetylacetonato), may be described as a derivative of the Fe(acac)<sub>3</sub> complex in which two bidentate acac ligands have been replaced by two Cu(Mesalen) molecules acting as bridging bidentate ligands. Such structures have been described previously by Sinn and co-workers, who reported adducts of

Cu(salen) with divalent metal complexes.<sup>7</sup> At present, the  $[\text{2Cu-Fe}]$  compound has not been obtained in crystalline form suitable for X-ray structure analysis. However, the combination of magnetic susceptibility and EPR and Mössbauer spectroscopy techniques clearly demonstrates the presence of exchange coupling between metal atoms, reveals certain electronic properties of the molecule, and allows predictions of structural features to be made.

### Experimental Section

**Synthesis.** Cu(Mesalen) (0.003 mol) was dissolved in 250 mL of dichloromethane, and the solution was mixed with Fe(acac)<sub>3</sub> (0.0005 mol) and Fe(NO<sub>3</sub>)<sub>3</sub>·9H<sub>2</sub>O (0.001 mol) dissolved in 50 mL of methanol. A dark purple solution resulted, which was then heated and stirred for 2 h at 40 °C. The solution was allowed to cool at room temperature, and a brown-black precipitate was obtained after 2-3 h. The precipitate was filtered, washed with dichloromethane, and dried under vacuum. Anal. Calcd for C<sub>41</sub>H<sub>43</sub>N<sub>6</sub>O<sub>12</sub>Cu<sub>2</sub>Fe·0.5CH<sub>2</sub>Cl<sub>2</sub>·0.5H<sub>2</sub>O: C, 47.6; H, 4.3; N, 8.03; Cl, 3.39; Cu, 12.15; Fe, 5.34. Found: C, 47.43; H, 4.26; N, 8.16; Cl, 3.56; Cu, 11.96; Fe, 5.34.

**Infrared Spectra.** The complex was examined by standard IR methods to determine changes in bands of the reactant metal complexes and to determine characteristic bands of the trinuclear cluster; see below.

**Magnetism.** The magnetic measurements employed polycrystalline samples weighing about 4 mg and yielded the results shown in Figure 1. The experiments utilized a variable-temperature (4.2-300 K) Faraday-type magnetometer equipped with an Oxford Instruments continuous-flow cryostat. A negligible dependence of the susceptibility on magnetic field was observed at room temperature. The susceptibility was corrected for diamagnetism, estimated at  $-535 \times 10^{-6} \text{ cm}^3/\text{mol}$ .

**EPR.** The polycrystalline powder spectra (Figure 2) were recorded at X-band with use of a Bruker ER-200D spectrometer, also equipped with an Oxford Instruments continuous-flow cryostat (4.2-300 K).

**Mössbauer Spectroscopy.** The Mössbauer data (Figure 3) were obtained with a constant-acceleration spectrometer and source of <sup>57</sup>Co

- (1) (a) Université de Paris-Sud. (b) Oregon State University.
- (2) Gunter, M. J.; Mander, L. N.; Murray, K. S.; Clark, P. E. *J. Am. Chem. Soc.* **1981**, *103*, 6784-6787 and references within.
- (3) Landrum, J. T.; Hatano, K.; Scheidt, W. R.; Reed, C. A. *J. Am. Chem. Soc.* **1980**, *102*, 6729.
- (4) Dessens, S. E.; Merrill, C. L.; Saxton, R. J.; Ilaria, R. L.; Lindsey, J. W.; Wilson, L. J. *J. Am. Chem. Soc.* **1982**, *104*, 4357-4361.
- (5) Morgenstern-Badarau, I.; Georget, P.; Julve, M., submitted for publication in *Inorg. Chim. Acta*.
- (6) Journaux, Y.; Kahn, O.; Zarembowitch, J.; Galy, J.; Jaud, J. *J. Am. Chem. Soc.* **1983**, *105*, 7585-7591.

- (7) O'Connor, C. J.; Freyberg, D. P.; Sinn, E. *Inorg. Chem.* **1979**, *18*, 1077-1078 and references within.